The Morphological, Clinical and Radiological Outputs of the Preclinical Study After Treatment of the Osteochondral Lesions in the Porcine Knee Model Using Implantation of Scaffold Based on the of Calcium Phosphate Biocement

Katarína Vdoviaková [1]*, Ján Danko [1], Lenka Krešáková [1], Veronika Šimaiová [1], Eva Petrovová [1], Jaroslav Novotný [2], Zdeněk Žert [3], Filip Koľvek [3], Igor Valocký [3], Maroš Varga [4], Tatiana Špakovská [4], Jozef Pribula [4], Miroslav Gašpárek [5], Mária Giretova [6], Radoslava Štulajterova [6] and Ľubomír Medvecký [6]

[1]Department of Morphological Disciplines, University of Veterinary Medicine and Pharmacy in Kosice, Kosice, Slovakia, [2]Swine Clinic, University of Veterinary Medicine and Pharmacy in Kosice, Kosice, Slovakia, [3]Equine Clinic, University of Veterinary Medicine and Pharmacy in Kosice, Kosice, Slovakia, [4]Hospital AGEL Kosice-Saca, Kosice, Slovakia, [5]Department of Engineering Science, University of Oxford, Oxford, United Kingdom, [6]Division of Functional and Hybrid Systems, Institute of Materials Research of SAS, Kosice, Slovakia

The symptomatic full-thickness cartilage lesions or cartilage degeneration leads to the destruction of the normal chondral architecture and bone structure in affected area, causes the osteoarthritis, and general damage to the health. Knee joints are most frequently affected by this condition. The permanent damage of the articular cartilage and subchondral bone has motivated many scientists and clinicians to explore new methods of regeneration of osteochondral defects, such as novel materials**.** We studied the potential of the biocement based on calcium phosphate consisting of a mixture of four amino acids (glycine, proline, hydroxyproline and lysine) in the regenerating process of the artificially created osteochondral defect on the porcine medial femoral condyle in the stifle joint. The mass ratio of the amino acids in biocement CAL was 4:2:2:1. The Ca/P ratio in cement was 1.67 which correspond with ratio in hydroxyapatite. We compared the results with spontaneous healing of an artificially created cyst with that of the healthy tissue. The animal group treated with biocement paste CAL presented completely filled osteochondral defects. The results were confirmed by histological and radiological assessments, which have shown regenerated chondral and bone tissue in the examined knee joints. Macroscopic evaluation showed that neocartilage was well integrated with the adjacent native cartilage in animal group with biocement CAL, compared with healing of the artificial cyst, where treated cartilage surfaces were visibly lower than the surrounding native cartilage surface and a border between native and restored tissue was apparent. The qualitative assessment of the implant histology specimens showed full regeneration of the hyaline cartilage and subchondral bone in animals with biocement CAL. The artificial

cyst group showed remarkable fibrillation. The detailed MRI analysis of cross-section of osteochondral defect confirmed the complete cartilage and subchondral bone healing where the thickness of the regenerated cartilage was 1.5 mm. The MRI imaging of defects in the artificial cyst group showed incomplete healing, neo cartilage tissue reduced up to 50%.

1 INTRODUCTION

The current fast lifespan emphasizes the need to bring a new trends and challenges in the treatment of bone and cartilage defects, as well as the development of new healing methods and biomaterial substitutes of cartilage and bone in view of minimally invasive surgical procedures and enhancing of healing process in affected site. From the point of view biomaterials, the first requirement represents the optimal filling of irregular and complex-shaped defects in the human population (Mano and Reis, 2007). Damage in the form of individual chondral or osteochondral lesions accounts for 67% of all arthroscopies (Widuchovski et al., 2007) and the injury of the articular cartilage, inflammatory and non-inflammatory diseases, irregular cartilage surface, symptomatic full-thickness cartilage lesions or degeneration of the cartilage results in the destruction of the normal chondral architecture as well as the bone structure in affected area and finally causes the osteoarthritis (Maglio et al., 2019). The osteoarthritis is a degenerative joint disease with typical symptoms (redness, swelling, heat, effluent, painfulness), loss of articular cartilage, narrowing of the joint space, inflammation, changes in synovium and bone structure (subchondral bone remodeling, cysts or osteophytes formation, sclerosis and lesions of the bone marrow (Macfadyen et al., 2019). However, early diagnosis by conventional radiography (X-ray), which allows indirect evaluation of damaged cartilage and bone, or imaging of hyaline cartilage by non-invasive method, direct magnetic resonance imaging (MRI examination), are good choices for capturing joint damage, traumatic or degenerative cartilaginous lesions in terms of current therapeutic options (Rodrigues and Camanho, 2010). In the body, the knee joints belong to the most frequently affected joints. The permanent damage of the articular cartilage and subchondral bone (osteochondral defects) represents an interesting opportunity for the scientists and clinicians to explore new methods or special materials for regeneration of osteochondral defects (Chu et al., 2010). The surgical approaches as mosaicplasty, arthroscopic microsurgery, chondrocyte implantation, or others, which were used for chondral or osteochondral defects therapy frequently failed due to incomplete fibrous or fibrocartilage tissue formation (Ozmeric et al., 2014). Currently, there are many methods and processes using different materials for treatment of cartilage lesions or bone. Meng et al. (2020) described in their review article different animal models, as a small, laboratory animals (rat, rabbit) and large, domesticated animals (dog, pig, sheep, goat, horse) of the osteochondral defect and possibility of the treatment using of the

different biomaterials ((osteochondral allograft, different types of scaffolds with MSC, transplantation/autologous cartilage chips, bone marrow derived cell concentrates, Hyaluronic acid in various forms). Authors used several locations (trochlear and patellar groove of the femur, femoral condyles) and different endpoints of the treatment (from 6 weeks to 24 months). The research of the osteochondral defects in rabbits with using of combination of biomaterials (chitosan) and cartilage promotive drug (icariin-conditioned serum) showed regenerative potential of this treatment method (ZhangMing et al., 2020). The suitable scaffolds for clinical use should be biodegradable, mechanically stable, noncytotoxic and ought to temporarily function as a support for the cells or other additives to facilitate the appropriate repair processes (Dhollander et al., 2012). Cement materials on the base of calcium phosphate have many interesting properties such as biocompatibility, bioresorbability, moldability, ability to support osteoconduction, osteoinduction and osseointegration, absence of any by-products during the process of metabolism and big potential for the replacement by new chondral and bone tissue after orthopedic surgery (Ambard and Mueninghoff, 2006). Scaffolds on the base of calcium phosphate biocement was studied in a bone structure regeneration, where it exhibited excellent biocompatibility and osteoconductivity (Cancedda et al., 2007), a similar type of biomaterial on the same base was described in small laboratory animals like a rabbit for treatment of chondral lesions on femoral condyle (Bernstein et al., 2013). The healthy articular cartilage is characterized by a smooth, glistening, bluish durable surface, and is largely responsible for the absorption of impact forces, and the ability to withstand high compressive forces. It has the ability to manage weight bearing with support of subchondral bone and facilitates bone movement (Junqueira and Carneiro, 2005; Maglio et al., 2019). The subchondral bone composed of water, hydroxyapatite and glycoproteins (type I and V collagen) is responsible for bone outer shape and appropriate biomechanical conditions for the development of cartilage at the physiological conditions in the knee joint. The articular cartilage is well integrated with underlying subchondral bone. Therefore, during the therapy of the chondral defects this bone structure should not be neglected (Deng et al., 2019). The hyaline cartilage is highly hydrated and specific connective tissue due to its composition. It does not have its own blood supply, network of nerves or lymphatic drainage (Reinholz et al., 2004; Malda et al., 2019). Experimental, preclinical animal models with artificially created osteochondral lesions that were studied include laboratory animals (Bauer et al., 2017), dogs (Salkeld et al., 2016), small

ruminants (Yucekul et al., 2017) and horses (Vindas Bolanos et al., 2017). The healing of the osteochondral defects in animal models is significantly influenced by differences in metabolism, diet, type of the digestive system and the levels of specific hormones relative to the levels in humans (Jainudeen et al., 2000). The selection of a suitable animal model is a prerequisite for connection between development of the new biomaterials and their application in clinical practice as well as for the proper evaluation of a degradability, biocompatibility, and interaction of biomaterials with cartilage and subchondral bone (Meng et al., 2020). It seems that the pig model (Large white pig) represents a more appropriate animal model for the study of osteochondral defect, compared to humans, because the pigs have similar anatomical structure of the organs. The size of the porcine joints, their weight, and thickness of the articular cartilage are very similar to the human population compared to another animal model (Meng et al., 2020); consequently, the pig model was used in this work. The porcine cartilage thickness is 1.5–2.0 mm thick Ahern et al., 2009) in the medial femoral condyle, while in humans, the thickness varies from 1.65 to 2.65 mm (Shepherd and Seedhom, 1999). The smallest chondral lesion that requires treatment in humans should be at least 10 mm in diameter (Chu et al., 2010). The cartilage defect with critical size of 6 mm heals spontaneously in the large pigs (Ahern et al., 2009). The purpose of this study was to investigate the potential of acellular calcium phosphate biocement in the regenerating process of the created osteochondral defect (diameter of 10 mm, depth of 10 mm) on the medial femoral condyle in large pigs. The repair ability of calcium phosphate biocement was compared to spontaneous healing of an artificial created cyst and natural cartilage and bone structure.

2 MATERIALS AND METHODS

2.1 Fabrication of Powder Cement Mixtures and Cement Samples

The tetracalcium phosphate/monetite/amino acid powder cement mixture (CAL) was prepared according to method showed in previous paper (Medvecký et al., 2021). Briefly, the tetracalcium phosphate [$Ca_4 (PO_4)_2O$, TTCP] was prepared by milling (Fritsch 5) of annealed an equimolar mixture of calcium carbonate ($CaCO_3$, analytical grade, Sigma-Aldrich) and dicalcium phosphate anhydrous (DCPA) ($CaHPO_4$ (Ph.Eur.), Fluka), at 1,450°C for 5 h. Consequently, the CAL was synthesized *in situ* by milling of TTCP with H_3PO_4/amino acid ethanolic solution (80% ethanol) with mass ratio of glycine:hydroxyproline:proline:lysine = 4:2:2:1 for 30 min. The Ca/P ratio in cement was 1.67 which correspond with ratio in hydroxyapatite. The cement pastes were prepared by mixing powdered CAL with 2% NaH_2PO_4 solution as hardening liquid and P/L ratio = 2.

2.2 Surgical Procedure in Porcine Model
2.2.1 Animals
The 5 months old Large White female pigs (breeding farm PD Agro Michalovce, Slovak Republic) were included as an implant

group ($n = 3$) and as an artificial cyst group ($n = 3$) for the study of the osteochondral defect treatment (**Table 1**). The mean body weight of the animals was 58.9 ± 5.88 g (mean ± SD). Pigs were selected as the animal model for the osteochondral defects because of their joint size, good cartilage thickness, ease of handling and availability. Animals were housed in the Swine clinic of the University of Veterinary Medicine and Pharmacy in Kosice (Kosice, Slovak Republic) and checked daily by qualified animal personnel. All pigs were fed with a standard diet and were given free access to water during the *in vivo* testing. The experiment received an official approval from the state authorities of the State Veterinary and Food Administration of the Slovak Republic (study No. 4650/17-221).
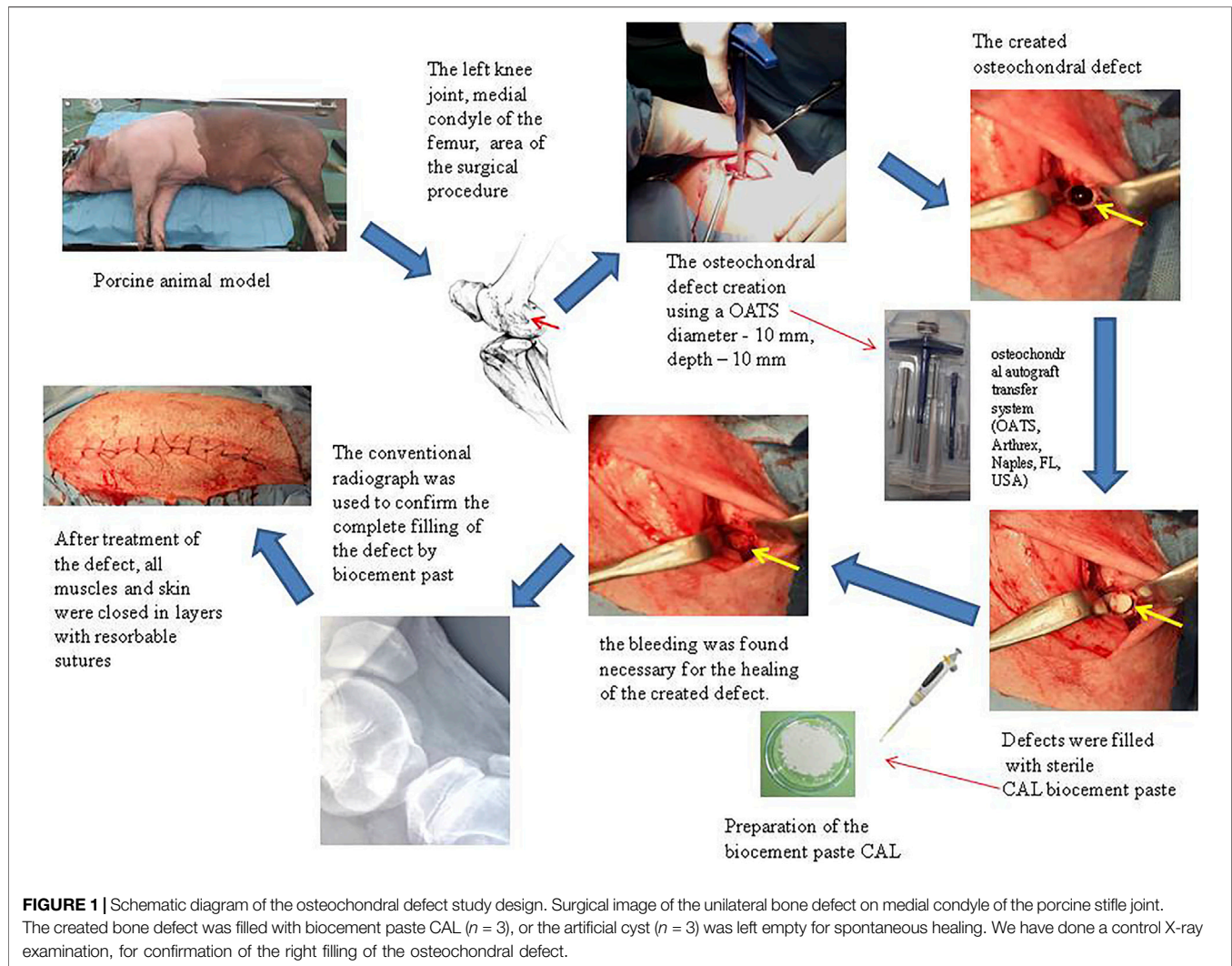
2.2.2 Anaesthesia
Before induction of a general anaesthesia, a permanent intravenous cannula was placed in the left auricular vein (*v. auricularis sinistra*). After premedication of the animals with a mixture of atropine 0.02 mg/kg body weight (Atropine sulphate 1 mg/ml solution for injection, Fatro s.p.a, Bologna, Italy), the azaperone 5 mg/kg body weight (Stresnil 40 mg/ml, Janssen Pharmaceutica, Beerse, Belgium) and butorphanol 0.02 mg/kg body weight (Butomidor 10 mg/ml, Richter Pharma, Wels, Austria) were administered intramuscularly. The general anaesthesia was established with thiopental 15 mg/kg body weight (Thiopental VUAB 1.0 g, VUAB Pharma a.s., Czech Republic) administered intravenously.

2.2.3 Unilateral Creation and Filling of Osteochondral Defects
The skin incision was made in the midline ranging from the medial patellar ligament (*lig. patellae mediale*) to the tibial tuberosity (*tuberositas tibiae*), distally, on the left stifle joint. An osteochondral defect (diameter of 10 mm, depth of 10 mm) was created on the high-weight-bearing medial femoral condyle (*condylus medialis*) using a commercially available osteochondral autograft transfer system (OATS, Arthrex, Naples, FL, United States) that allows defect creation with controlled diameter and depth. For stimulation of the artificial defect healing by bleeding from bone cavity, the perforation of subchondral bone to the desired defect depth was carried out. Defects in cartilage and subchondral bone were experimentally filled with sterile CAL biocement paste in the first experimental group (3 animals). The artificial cyst created in osteochondral defect was left empty for spontaneous healing in the second group (3 animals). We compared experimental groups (CAL biocement paste and artificial cyst) with the control group (the medial condyle of the right stifle joint) of pigs with native cartilage and bone. After treatment of the defect, all muscles and skin were closed in layers with resorbable sutures and covered by liquid aluminium wound bandage. We did not use splints, casts or immobilisation techniques with any animal. The conventional radiographs of the lateral view porcine knee joint were used to confirm the complete filling of the defect by biocement paste. Animals were residing individually in a solid pen, on straw bedding, after the implantation. Pigs were allowed immediate full weight bearing on their limbs and returned to normal activity.

TABLE 1 | The details of the animals groups used in our study.

Animals	Weight of the animals (kg)	Number of animals (ks)	Material	Place of defect	Size of defect (mm)	Euthanasia of animals after (months)
1. Group	58.9 ± 5.88 g	3	CAL biocement	Medial femoral condyle of the left limb	10 × 10	3
2. Group	58.9 ± 5.88 g	3	Artificial cyst	Medial femoral condyle of the left limb	10 × 10	3

FIGURE 1 | Schematic diagram of the osteochondral defect study design. Surgical image of the unilateral bone defect on medial condyle of the porcine stifle joint. The created bone defect was filled with biocement paste CAL ($n = 3$), or the artificial cyst ($n = 3$) was left empty for spontaneous healing. We have done a control X-ray examination, for confirmation of the right filling of the osteochondral defect.

Schematic diagram of the osteochondral defect study design described **Figure 1**.

2.2.4 Postoperative Care

Postoperative care consisted of application of antibiotic prophylaxis with repeated shot doses of broad-spectrum antibiotics oxytetracycline dihydrate 1 ml/10 kg body weight (Alamycin LA a.u.v., Norbrook, Newry, United Kingdom), intramuscularly once per every second day for 7 days, and from repeated injections of non-steroidal anti-inflammatory drug flunixin meglumine 2.2 mg/kg body weight (Flunixin a.u.v., Norbrook, Newry, United Kingdom), intramuscularly once a day for 7 days. The animals were monitored daily in the postoperative period, until the end of the experiment. The following parameters were evaluated: state of general health, body temperature, faecal consistency, degree of limb pain, the surgical wound, signs of inflammation (redness, swelling, heat, discharge, pain) and a grade of the degree of lameness. The animals were regularly monitored and clinically examined (assessment of general health, body temperature, degree of pain and lameness).

TABLE 2 | Macroscopic evaluation of the cartilage repair according to ICRS (Van den Borne et al., 2007).

Cartilage repair assessment system	Characteristics and points
Degree of defect repair	100% - 4 75% - 3 50% - 2 25% - 1 0% - 0
Integration to border zone	Complete integration - 4 Demarcating border <1 mm - 3 3/4th of graft integrated - 2 1/2 of graft integrated - 1 From no contact to 1/4th of graft integrated - 0
Macroscopic appearance	Intact smooth surface - 4 Fibrillated surface - 3 Small, scattered fissures or cracs - 2 Several, small or few but large fissures- 1 Total degeneration of grafted area 0
Overall repair assessment	Grade I: normal - 12 Grade II: nearly normal - 11–8 Grade III: abnormal - 7–4 Grade IV: severely abnormal - 3–1

2.2.5 Euthanasia of Animals and Speciment Retrieval

Animal euthanasia was performed 3 months after the implantation surgery. After sedation of the animals with azaperone 2 mg/kg body weight (Stresnil 40 mg/ml Janssen Pharmaceutica, Beerse, Belgium) intramuscularly, euthanasia was established intravenously with thiopental 90 mg/kg body weight (Thiopental VUAB 1.0 g, VUAB Pharma a.s., Czech Republic).

After removing the muscles from the left pelvic limbs, the knee joint capsules were opened for macroscopic evaluation of the appearance of the cartilage surface. The cartilage surface was examined, digitally photographed and harvested for documentation. The created osteochondral defects sites were analyzed macroscopically, histologically, immunohistochemically and by radiographic imaging. The medial condyle of the right knee joint was used as a positive control.

2.3 Assessment of Tissue Regeneration

2.3.1 Macroscopic Evaluation

The cartilage defect site and adjacent tissue was assessed after removing the soft tissues. The macroscopic evaluation included the observation of neocartilage surface roughness, colour, opacity, translucency, consistency, defect filling, edge integration with adjacent tissue and the comparison with original, physiological surrounding cartilage. The articular surfaces of the femur distal epiphysis and tibia proximal epiphysis, the synovial membrane and knee joint capsule were examined for signs of inflammation and abnormalities (osteophytes). The new repair cartilage (animal group with biocement and artificial cyst) was scored using rules of the International Cartilage Repair Society (ICRS) scoring system for cartilage repair (Van den Borne et al., 2007); (**Table 2**).

TABLE 3 | Visual Histological Assessment of cartilage repair according ICRS, modified from the scale described by (Mainil-Varlet et al., 2003).

Feature	Points
Surface	Hyaline cartilage - 3 Hyaline cartilage/fibrocartilage - 2 Fibrocartilage - 1 Fibrous tissue - 0
Matrix	Columnar - 3 Columnar/clustery - 2 Clustery - 1 Individual cells/disorganized - 0
Cell distribution	Predominantly viable - 3 Partially viable - 1 Less than 10% viable - 0
Cell viability	Predominantly viable - 3 Partially viable - 1 Less than 10% viable - 0
Subchondral bone	Normal - 3 Increased remodeling - 2 Bone necrosis/granulation tissue - 1 Detached/fracture/callus at base - 0
Cartilage calcification	Normal - 3 Abnormal/inappropriate location - 0

2.3.2 Histological and Immunohistochemical Analysis

The specimens including the defect area of the regenerated tissue site was obtained by collecting a 10 mm diameter and 10 mm long bone cylinder using the osteochondral autograft transfer system (OATS, Arthrex, Naples, FL, United States), fixed in neutral formalin per 1 week. Following fixation, the specimens were decalcified in chelation per 1 month, dehydrated through a series of 70–100% ethanol and embedded in paraffin. Embedded specimens were serially

sectioned at 7 μm thickness in the sagittal plane, mounted on slides and prepared for staining with Hematoxylin and eosin (H&E), Alcian Blue and Picrosirius red. The physiological articular cartilage sections from the medial condyle of the right knee joint were used as reference positive controls.

Primary antibody Rabbit polyclonal anti collagen antibody (Abcam) and a secondary antibody in DB DET SYS kit (Biotech) according to the instructions and visualization was used for immunohistochemical detection of collagen II process was performed with DAB (3,3′-diaminobenzidine) (DAKO) substrate. Light microscope (Olympus CX 23) was used for the examination and evaluation of the histological samples.

The quality of the repair cartilage was evaluated with the scale of the ICRS Visual Histological Assessment based on these parameters: cartilage surface and matrix, cell distribution and viability, subchondral bone and cartilage mineralization (Mainil-Varlet et al., 2003); (**Table 3**).

2.3.3 Radiological Analysis

Following a post-surgical period of 3 months, the conventional radiographs (x-ray analysis) and magnetic resonance imaging (MRI) of the left porcine knee joints after euthanasia were carried out to assess regeneration of the articular cartilage and subchondral bone tissue. We performed the x-ray analysis in the lateral view of the knee joint with x-ray (Philips Digital Diagnost, Delft, Netherlands). MRI examination of the pig knee joints in the single acquisition plane, in sagittal plane was obtained using an intended Zenith solenoid knee coil with PD FS sequence, because the articular cartilage is best visualized in this sequence (TR 3805.0 ms, TE 36 ms) with ultra-high resolution and slice thickness of 3.5 mm with MRI (1.2 T Hitachi Oasis, Open system, Hitachi Medical Systems Holding AG, Tokyo Japan). All MR images were transferred to a network of TOMO CON PACS and analyzed using dedicated image processing Tatra Med Software.

3 RESULTS

3.1 Macroscopic Evaluation

The macroscopic examination provided a preliminary evaluation of the osteochondral defect repair. In the monitoring period of 3 months after biocement applying, no significant differences in the mobility of the animals, except three pigs (one animal from implant group and two pigs from artificial cyst group) with observed macroscopic signs of inflammation in the defect site were recorded. In these animals, the first degree of lameness was found for 1 week.
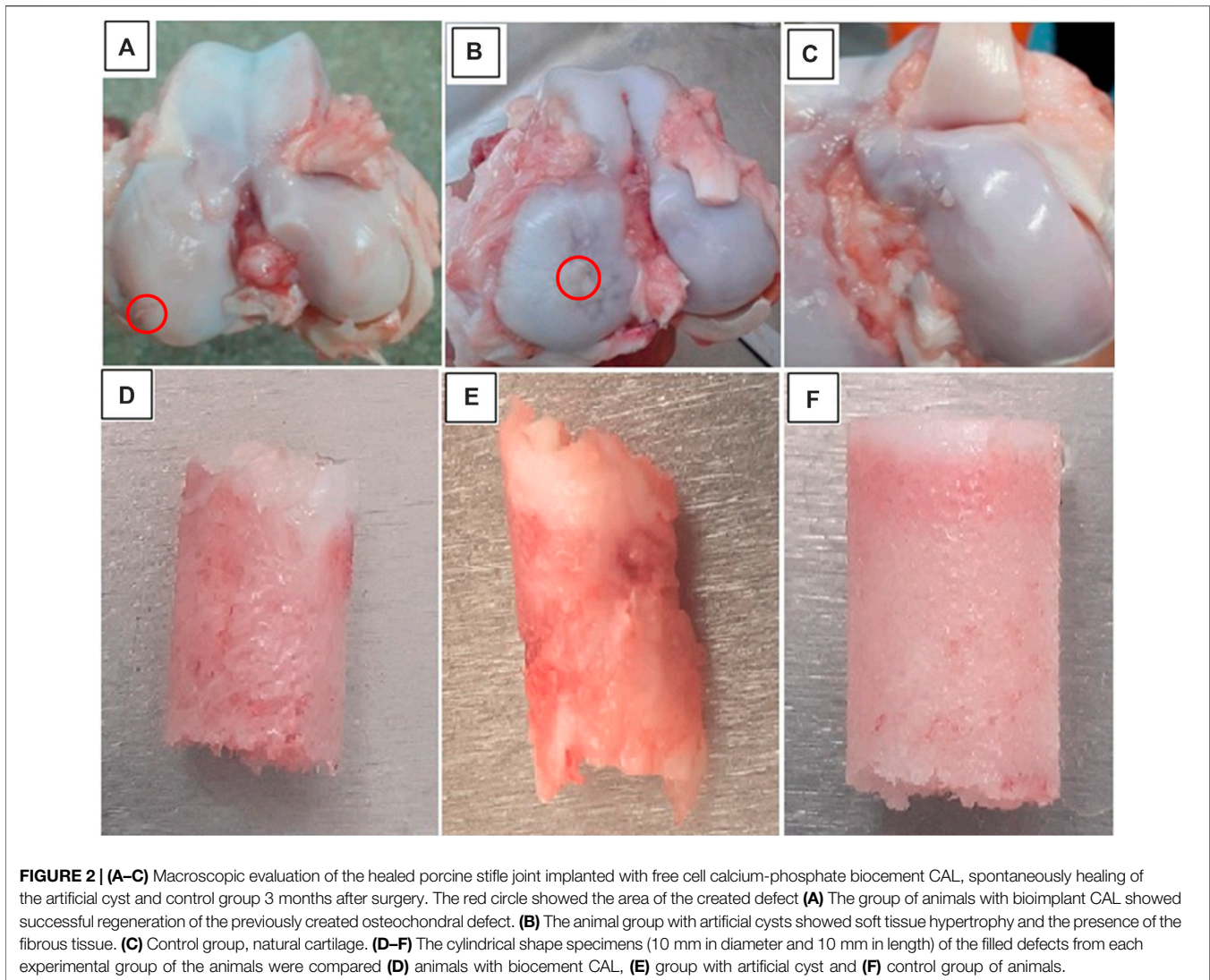
The evaluation of the functional status of all examined animals did not show deviations from normal. After opening the knee joint, there was no observation of abrasions on the articular surfaces and inflammation of the synovial membrane as well as the adjacent joint tissues. The defect site was visible macroscopically on studied stifle joints (animal group with biocement and artificial cyst), but healing time differences when compared to physiological cartilage have disappeared. Regenerated tissue of the neocartilage in the defect site was

observed in all experimental animals treated with biocement paste. The visual observation *in situ* of defects verified the high quality of the new tissue 3 months after application of biocement. Macroscopic evaluation showed that neocartilage was well integrated with the adjacent native cartilage in the biocement group. The neocartilage began to form from the edge and followed to the centre of the defect. This healing process resulted in uniform defect filling with tissue characterized by a fairly smooth, homogeneous, glistening bluish surface, close to adjacent healthy articular cartilage (**Figure 2C**). The height of the neocartilage surface was approximately at the same level as adjacent cartilage (**Figure 2A**). Treated cartilage surfaces were visibly lower than the surrounding native cartilage surface; a border between native and restored tissue was apparent in experimental animals with artificial cyst after healing period. In this experimental group, the healing of a rough cartilage surface was evidenced and a coverage degree was verified to be repaired for 50%. Some samples of the artificial cysts were noted fissures near the centre or depressions of the cartilage repair tissue (**Figure 2B**). The treated According to rules of the International Cartilage Repair Society (ICRS), the overall repair process in the biocement group was normal (12, grade I) contrary to abnormal process (6, grade III) in the experimental group with artificial cyst. The cylindrical shape specimens (10 mm in diameter, 10 mm in length) from each experimental group pointed out the macroscopic features inside the previous defect (**Figures 2D–F**).

3.2 Histological and Immunohistochemical Analysis

Histological evaluation of tissues from the CAL biocement group confirmed the macroscopic results. The qualitative assessment of the implant histology specimens showed full regeneration of the hyaline cartilage and subchondral bone. Neocartilage integration showed excellent interconnection with the native cartilage and the thickness of regenerated cartilage was the same as adjacent cartilage and comparable with the control sample (**Figure 3C**). The cartilage surface was relatively smooth and specimens did not show the cement residue. The biocement was entirely reabsorbed and a defect was completely filled by new regenerated tissue. Structure of neocartilage was homogeneous without fissures or cleft formation. In the histological specimens, all layers of cartilage were very well visible with typical cell density, ordering and morphology of the chondrocytes in the synthesized matrix (**Figure 3A**). A relatively high number of the flattened, elongated chondrocytes arranged parallel to the cartilage surface were located in the tangential zone. In the transitional zone, there were detected low density chondrocytes with typical spherical morphology. For this zone was characteristic markedly staining with both Picrosirius red and Safranin Q. The uniform intensive staining of the specimens with Picrosirius red pointed out on the high content of the collagen (**Figure 3D**) comparable to control group (**Figure 3F**).

The radial zone was composed of small spherical chondrocytes arranged to columnar form, perpendicularly to the articular surface. The intensity of Safranin Q staining indicated the

FIGURE 2 | (A–C) Macroscopic evaluation of the healed porcine stifle joint implanted with free cell calcium-phosphate biocement CAL, spontaneously healing of the artificial cyst and control group 3 months after surgery. The red circle showed the area of the created defect **(A)** The group of animals with bioimplant CAL showed successful regeneration of the previously created osteochondral defect. **(B)** The animal group with artificial cysts showed soft tissue hypertrophy and the presence of the fibrous tissue. **(C)** Control group, natural cartilage. **(D–F)** The cylindrical shape specimens (10 mm in diameter and 10 mm in length) of the filled defects from each experimental group of the animals were compared **(D)** animals with biocement CAL, **(E)** group with artificial cyst and **(F)** control group of animals.

highest content of proteoglycans typical for this zone (**Figure 3G**) and comparable with the control group (**Figure 3I**). At the interface between the radial zone and the zone of the calcified cartilage was a well visible tidemark. A more detailed analysis showed a low cell population in a zone of calcified cartilage with hypertrophic chondrocytes. The zone of the calcified cartilage played an important role in interconnection between the cartilage and subchondral bone and was followed by a highly mineralized layer of the subchondral cortical zone known as subchondral plate and the subchondral trabecular bone. Both bone tissues serve as support for other overlying cartilage layers. No differences were found between the newly formed subchondral bone and the origin native tissue. Immunohistochemical analysis of a sample from an osteochondral defect treated with CAL biocement showed the presence of collagen II in all cartilage zones (**Figure 4A**) as well as in the pericellular matrix of chondrocytes (**Figure 4B**).

We proved with histological examination the presence of the healthy, adults chondrocytes which playd with their mechanical environment and the very important role for the right moving in the artcular joints. The metabolic acivity of the chondrocytes was affected by the accumulation of the mechanical signals of the articular cartilage.

The artificial cyst group showed remarkable fibrillation of the articular cartilage surface, which was irregular with flaking layers. It was visible that the thickness of the tissue was different in the cross section. There was an observation of good integration between newly formed and origin tissues. The neocartilage contained a lower amount of hyaline-like cartilage due to combination of the hyaline and fibrous cartilage with the acellular regions in the layers (**Figure 3B**). Moreover it had a lower cell density than the adjacent cartilage. The intensity of color after Picrosirius red staining was much lower in the artificial cyst group which revealed reduction in the content of collagen (**Figure 3E**). The individual layers of the chondral part in defect
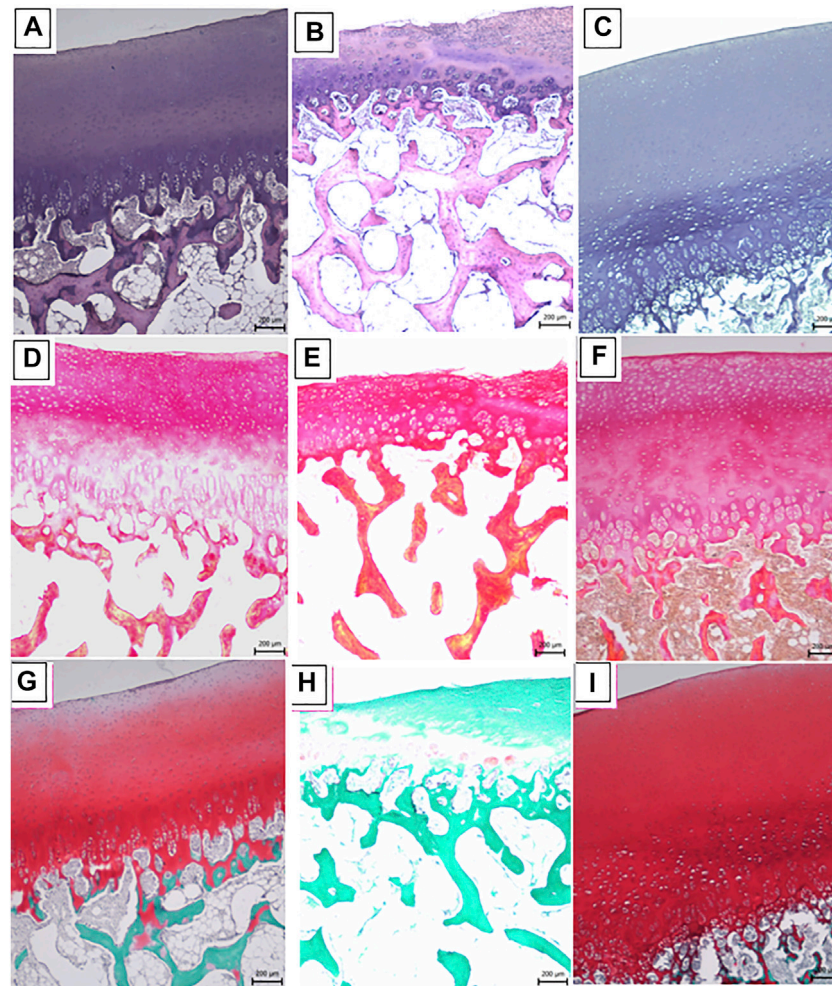
FIGURE 3 | (A–C) H & E staining **(A)** The regenerated cartilage from the free cell implantation biocement CAL group was similar to the native hyaline cartilage with typical chondrocytes in each layer. **(B)** The group with artificial cyst showed remarkable fibrillation of the articular cartilage surface and formed less hyaline-like cartilage or combination of the hyaline and fibrous cartilage. **(C)** The normal knee joint cartilage showed native hyaline cartilage chondrocytes morphology. **(D–F)** Picrosirius red staining (D) The uniform, intensive staining of the specimens with Picrosirius red pointed out on the high content of the hyaline collagen architecture in animal groups with biocement CAL. **(E)** The artificial cyst group showed significantly less this staining, due to the low content of collagen fibers. **(F)** The control group presented a normal intensity of Picrosirius red staining. **(G–I)** Safranin Q staining **(G)** The intensity of Safranin Q staining indicated the highest content of proteoglycans in animal group with biocement CAL, typical for the radial zone. **(H)** The individual layers of the chondral part in the artificial cyst defect showed a significant less Safranin Q staining of GAG in the extracellular matrix. **(I)** The animal group with control sample showed the intensity of the Safranin Q staining typical for the native hyaline cartilage.

showed signs of cartilage degradation with chondrocyte cluster formation as well as less intense Safranin Q staining of GAGs in the extracellular matrix (**Figure 3H**). The superficial zone was characterized by the fibrous tissue, composed of fibrocytes placed parallel to the surface of the joint. It was found a small volume of morphologically typical chondrocytes contrary to strong cell clustering in both the superficial and transitional zone of the cartilage. The partial clustering was observed in the radial zone and also identified the acellular region in the transitional zone. In the distal part of the radial zone, small spherical chondrocytes were arranged in columnar orientation. The endochondral ossification conducted a formation of the new trabecular bone and the subchondral trabecular bone integrity was restored after 3 months from surgery. The ICRS Visual Histological Assessment

provided a quantitative comparison of the repair tissue of cartilage and bone in both experimental groups (group with biomaterial and artificial cyst), (**Figure 5**).

3.3 Radiographic Analysis

Conventional radiographic analysis (X-ray) and magnetic resonance imaging (MRI) were used for evaluation of treated osteochondral defects.

In the case of CAL biocement, the lateral radiographs showed the equal, lucent joint space narrowing and no formation of the osteophytes (**Figure 6C**) or deformity of the femur, condyles contours and tibia. Plain radiography allowed assessment of changes in the adjacent subchondral bone, the presence of the subchondral osteosclerosis and cyst. In the biocement group,
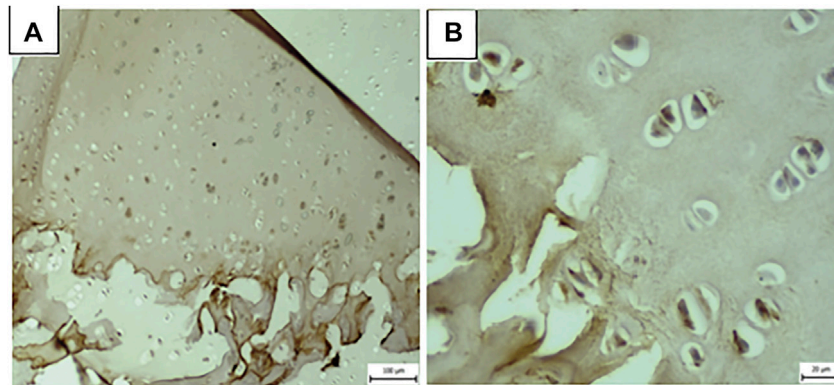
FIGURE 4 | Immunohistochemical staining **(A)** in the cartilage tissue representative sample in all cartilage zones, **(B)** as well as in the pericellular matrix of chondrocytes.
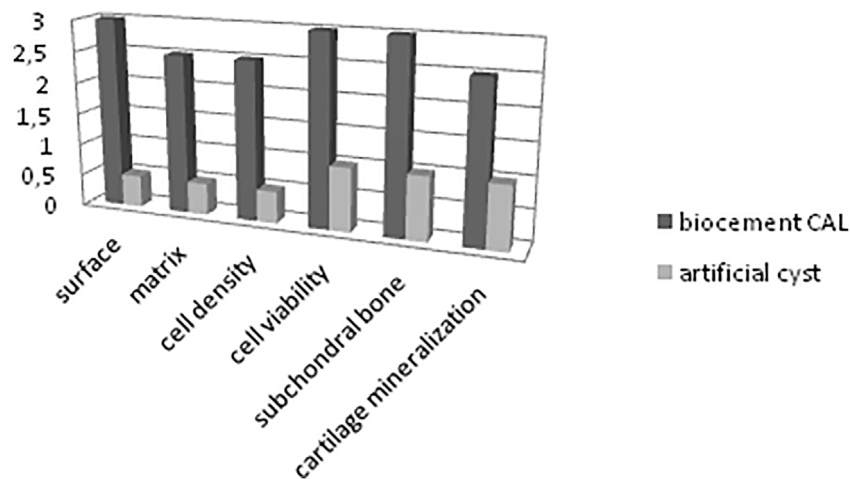
FIGURE 5 | The ICRS Visual Histological Assessment provided quantitatively comparison the repair tissue of the cartilage and bone in both experimental groups (biocement CAL group and artificial cyst group).

none pathological changes were revealed. The radiographs evaluation in the artificial cyst group pointed out the same, uniform joint space size between the epiphyses of the bones as well as no pathological changes occured on soft tissues (**Figure 6D**). The conventional radiography showed the presence of the bone cysts and partially healing of osteochondral defect (**Figure 6E**). The MR imaging of defect treated with biocement, showed a smooth articular surface of neocartilage with homogeneous structure and complete integration within surrounding articular tissue. The detailed analysis of cross-section of osteochondral defect confirmed the complete cartilage and subchondral bone healing in biocement group where the thickness of the regenerated cartilage was 1.5 mm. Besides, in all treated defects with biocement there was measurement of the intensity of the signal identical to adjacent articular cartilage and the complete integration of the new subchondral bone with native subchondral bone tissue was

found. The detail MRI analysis of the defect after therapy with biocement CAL shown the defect filling was on 100% and its location of the defect filling was in the whole area. The integration with surrounding tissue (oseal and subchondral tissue) was complete. The defect boundary (oseal and subchondral tissue) was very weakly indicated. The character of the newly formed subchondral bone was homogenous. The cover cartilage thickness at the level of the defect was uniform thickness, without apparent reduction, contour of the covering cartilage without significant irregularities or newly formed small defects (compared to the surrounding healthy cartilage). The structure of the covering cartilage at the level of the defect was only minimally inhomogeneous. The signal intensity (covering cartilage at defect level) was very discrete hyposignal in T1 v.o., almost iso signal in PD FS sequence compared to adjacent cartilage. The MRI examination showed, that after the osteochondral defect on the medial condyle of the femur with implantation of

FIGURE 6 | (A–B) High-resolution, PD FS sequence, SPACE sequence (TR/TE: 3805/36) to assess treated osteochondral defects, 3 months after surgery in sagittal plane MRI. The arrow shows the surgical area. **(A)** The osteochondral defect was filled completely by the new tissue in the animal group with biocement CAL. **(B)** In the group with artificial cysts, the bone defect region was not fully filled with bone structure, and the cartilage surface was visibly lower than surrounding native chondral tissue; a border between native and restored tissue was apparent. **(C–E)** Using standard radiographs, we obtained the required spatial resolution in the examined knee joint. **(C)** In the group with biocement paste CAL the lateral radiographs showed the equal, lucent joint space narrowing, no formation of the pathological structures in the stifle joint cavity. **(D)** The x-ray evaluation in the experimental artificial cyst group pointed out the uniform joint space size and **(E)** the presence of the bone cysts in some cases.

biocement CAL, on the sclerotization signs around the circumference of the axial effect, indicating the healing process and signs of regeneration (new formation) of the cartilage at the defect level, thickness, structure and signal intensity healthy cartilage. Thus, it is clear from above results that enhanced healing process in the knees treated with CAL biocement was verified as compared to artificial cysts group after 3 months from implant surgery and intensity was comparable to the control knees (**Figure 6A**). The rough articular surface with shallow superficial ulcerations and morphological imperfections such as fraying, fissuring or fibrillation without exposure of subchondral bone was found in the artificial cyst group. The MR imaging of defects in the artificial cyst group showed incomplete healing (neo tissue reduced up to 50%) after 3 months from surgery (**Figure 6B**). The origin cartilage thickness of neocartilage was identified on MR imaging only on the periphery of defect (chondral tissue reduced up to 50%). According to the tissue

analysis the incomplete healing characterized low signal intensity in the defect central part which was verified.

4 DISCUSSION

The complex physico-chemical properties of CAL cement were discussed in the previous article (Medvecký et al., 2021). Note that the analysis of properties clearly showed a significant reduction in compressive strength of the cement (down to 5 MPa in the wet state) after the addition of amino acids compared to tetracalcium phosphate/ monetite biocement without additives. In addition, a large amount of amino acids remained adsorbed on the surface of the formed nanohydroxyapatite particles in the cement, which effectively modified the morphology of its particles from needle-like to spherical, which is more suitable for cell adhesion and growth. The presence of amino acids in the cement suppressed the increase in pH

during setting of the cement, demonstrating the suitable buffering capacity of the amino acids in the cement. In addition, the porosity of CAL cement was relatively high (about 57%) and two pore fractions of different sizes were identified in the cement microstructure - larger micropores with a size of 10–15 μm and a main fraction with 1–3 μm micropores. Similarly, RT-qPCR analysis showed high stimulation of osteoblasts to express of the collagen I, OP, ON and ALP in CAL.In terms of collagen II production, the addition of glycine with a small supplementation of LYS or PRO in culture medium strongly induced the *in vitro* production of collagen II by chondrocytes (De Paz-Lugo et al., 2018). On the other hand, the PRO supplementation of medium had little but significant effect on *in vitro* collagen biosynthesis by fibroblasts, but nevertheless a strong positive effect of extracellular PRO on collagen biosynthesis was verified in case of insufficient endogenous PRO synthesis (Karna et al., 2020). We hypothesize that the mixture of amino acids in calcium phosphate cement promotes the differentiation of MSCs into chondrocytes by increasing collagen biosynthesis due to reduction in further endogenous synthesis of the corresponding amino acids required for collagen production by cells. In addition, the reduced mechanical properties of cements contribute to the differentiation of bone marrow stem cells into chondrocytes and the subsequent formation and growth of cartilage tissue.

The knee joint is the supporting structure of the pelvic limb. It resists tremendous impacts and loading of the articular cartilage and subchondral bone, but after long time, these factors can result in cartilage and bone tissue damage and may lead to the development arthritis or osteoarthritis. Many previous studies have reported that newly formed cartilage rarely has the same biomechanical properties as physiological hyaline cartilage. In the case of the deep osteochondral defects where the subchondral bone has been damaged, treatment strategies of those structures should also be considered (Interna et al., 2011). There are previous studies, which noted that the newly formed bone has the similar biomechanical properties as surrounding bone tissue, because the bone is dynamic structure getting constant remodelling. Each restoration of the fracture or bone defects treatment depends on using material treated area of the body and very important role has a type of ossification (Kim et al., 2020). Autogenous bone grafts constitute as a golden standard in therapy of the bone tissue (Wang and Yeung, 2017). Excellent properties like as osteoconductivity and osteoinductivity of the implants based on calcium phosphate as evidenced our results. In the osteochondral defect, the biocement paste CAL promoted a bone formation, remodelling and osteointegration, leading to enhanced repair of the subchondral bone defect. Therapy of deep osteochondral defects of the knee joint presents a big challenge for *in vivo* research aimed at optimizing healing techniques and methods (Lydon et al., 2019; Kresáková et al., 2021). In the current time between the normally using healing therapies of the stifle joint articular cartilage after the traumatic damages belong microfractures and the osteochondral autografts and allografts (Mathis et al., 2018). The treatment should include only minimally invasive surgical procedures and methods of marrow cells stimulation to support the progress of the formation of new tissue with the same properties as the physiological chondral tissue and bone structure (Carneiro et al., 2013). Scientists have been researching the role of different materials in the treatment of osteochondral lesions for many years. The properties of the

materials can greatly influence of the mechanical environment of the healing process in treatment osteochondral defects (Davis et al., 2021). It is possible to study various implants on the experimental animal models under physiological conditions, as they provide better understanding of the response in humans. Our study compared results from a treatment of the artificially created osteochondral defects (10 mm diameter and 10 mm depth) with special biocement and spontaneous healing of the artificial cysts with control healthy cartilage and subchondral bone, in the medial condyle of the left knee joint in the pig within 3 months. Ho et al. studied porcine osteochondral defects in two areas, in the high-load bearing femoral condyle and in the low-load bearing trochlear groove. They found that better results were in the condyles, because mechanical stimulus had beneficial effects on the regeneration of the chondral and bone tissue. This study pointed to a close interaction between the articular cartilage and bone tissue, because the treatment of chondral defect was dependent on the underlying subchondral bone (Ho et al., 2010). The other investigation affirmed that differences of biomechanical properties between artificial tissue, biomaterials and subchondral bone in different animal species can be the reason for incomplete healing created defects (Archibald et al., 2002). Therefore we choose the medial condyle of femur for creation of the osteochondral defect in our study. Prior research has demonstrated that the use of the porcine model is more comparable with publications, which described other species of animals as a model (Ahern et al., 2009; Pilichi et al., 2014; Vilela et al., 2015; Kresáková et al., 2021). Pearce et al. (2007) stated that the bone composition, micro- and macrostructure, remodelling and the bone density in the pig is very similar to that with humans. Shimomura et al. (2010) and Archibald et al. (2002) affirm that due to the thickness of the porcine articular cartilage on medial femoral condyle being comparable with chondral layer in humans, this animal model should be used for the study and evaluation of the healing the chondral or osteochondral defects. The thickness of the articular cartilage changes depending on the age and varies among the species. The younger animals have thicker cartilage layers than the older ones, but the content of GAG and flexibility are lower in immature cartilage. The biomechanical properties of the chondral structures are influenced by the content of GAG too (Shimomura et al., 2010). As evidenced by our results of staining, the highest intensity of Safranin Q (the proof of the highest content of proteoglycan) was found in the radial zone. The properties of the chondral cells (morphology, density) and another component in all layers were comparable with hyaline cartilage. Our study confirmed that the subchondral bleeding strategy, with drilling marrow stimulating techniques, is very important for the formation and repair of the chondral and bone tissue, because the blood from the bone marrow contains mesenchymal stem cells, which differentiate into osteoblasts and chondroblasts. On the similar principle functions the surgical method of the microfractures, where is recruitment of stem cells by drilling the subchondral bone to allow bone marrow to flow into the osteochodral defect site and initiate healing (Yen et al., 2008). Many previous studies pointed out, that the bone marrow stimulation induced the bleeding, which in the defect site supported a blood clot formation, composed of the mesenchymal stem cells (MSC) that facilitated tissue regeneration and served as template for the matrix formation (Smith et al., 2005;

Madry et al., 2017; Zlotnick et al., 2021). This is also evidenced by other research results that consisted of cell tracing using iron oxide particles in cartilage defects without drilling into the subchondral bone. This research found that approximately 30% of the cells in the new cartilage tissue at 12 weeks were coming from the transplanted population, because the majority of cells migrated from subchondral bone (Blanke et al., 2009). Many different chondral lesions have been treated by the implantation techniques using chondrocytes, but these treatments failed, because mechanical stability was not provided (Matricali et al., 2010). Other authors noted, that after using poly-LD-lactic scaffold or polycaprolactone nanofibrous scaffold with seeded cells (chondrocytes, MSCs), were repaired only defects of cartilage, but bone structure did not have properties of the subchondral bone. There was only soft tissue or cartilage instead of bone structure (Pulliainen et al., 2007). In scaffolds seeded by cells, a major problem is hypertrophy of these cells (Bernstein et al., 2013). Currently, the osteochondral damage therapy focuses on replacement of damaged cartilage and bone by special biomaterials, which lead to regeneration of the chondral and bone tissue (Kon et al., 2012). According to some authors, the part of scaffolds that remained in bone neither degraded nor slowed down the treatment process (Leja and Lewandowicz, 2010). The macroscopic, microscopic assessment and radiographic analysis demonstrated the successful regeneration of the treated osteochondral defects in a porcine knee joint using cell free calcium phosphate scaffold CAL in our research. Both types of tissues in the site healed osteochondral defects had typical features of the chondral and bone tissue. In comparison, several publications described artificial scaffold, which can be inappropriate to regenerate articular cartilage, or only lead to fibrocartilage formation (Higa et al., 2017; Murata et al., 2018; Tamaddon et al., 2020). The results of some experiments indicate that combination of special additives (erythropoietin, bone marrow aspiration concentrate) with scaffold could help improve the healing of osteochondral defects (Betsh et al., 2014). The basis of many studies of tissue engineering methods was bone marrow cells collection, isolation, cultivation and their application separated or embedded in biomaterials into the created defects. Each of these steps required at least two surgery procedures (Liua et al., 2017; Bozkurt et al., 2019). According to the results of the cartilage biomechanical research of Archibald, et al., pigs, as animal models used for creation of chondral or osteochondral defects, have 2–5 times stronger and stiffer subchondral bone than humans do (Archibald et al., 2002). Our objective was to only employ a single surgical procedure, where we created a full-thickness osteochondral defect, based on deeper drilling to the subchondral bone, allowing for the supply of the blood from the bone marrow, together with its individual components necessary for regeneration processes. We also analyzed the results of our study with radiographic methods, which confirmed the findings of the previous evaluations (macroscopic, histological) of treated knee joints. In the animal group treated with biomaterial CAL, the defect filled by the new regenerated chondral and bone tissue and biocement was almost fully reabsorbed.

In conclusion we can state, that the important fact is that chondral and bone tissue are closely related. Therefore, during the treatment of the osteochondral defects, they must be considered as a complex of articular cartilage and subchondral bone, which have a very well organized tissue. The further research of the osteochondral lesions therapy should focus on improving modification of scaffolds, which will have the ability to create the physiological architecture of regenerated cartilage and subchondral bone, supporting their functional character and their mechanical properties. Although the bone marrow cells, growth factors and cytokines in scaffolds are important and interesting for the right repair processes in osteochondral lesions, their difficult storage, low survival rate of cells and instability of factors, makes use of the cell-free scaffolds for the therapy in the cartilage and subchondral bone preferable.

DATA AVAILABILITY STATEMENT

The original contributions presented in the study are included in the article/supplementary material, further inquiries can be directed to the corresponding author.

ETHICS STATEMENT

The animal study was reviewed and approved by State Veterinary and Food Administration of the Slovak Republic (study No. 4650/17-221).

AUTHOR CONTRIBUTIONS

FUNDING

ACKNOWLEDGMENTS

REFERENCES

Ahern, B. J., Parvizi, J., Boston, R., and Schaer, T. P. (2009). Preclinical Animal Models in Single Site Cartilage Defect Testing: a Systematic Review. *Osteoarthritis and Cartilage* 17 (6), 705–713. doi:10.1016/j.joca.2008.11.008

Ambard, A. J., and Mueninghoff, L. (2006). Calcium Phosphate Cement: Review of Mechanical and Biological Properties. *J. Prosthodont.* 15 (5), 321–328. doi:10.1111/j.1532-849x.2006.00129.x

Archibald, M., Runciman, J., Dickey, J., and Hurtig, M. (2002). Do animal Models Approximate the Subchondral Bone and Cartilage Characteristics of Humans? The 4th International Cartilage Repair Society. Toronto, 13–16.

Bauer, C., Jeyakumar, V., Niculescu-Morzsa, E., Kern, D., and Nehrer, S. (2017). Hyaluronan Thiomer Gel/matrix Mediated Healing of Articular Cartilage Defects in New Zealand White Rabbits-A Pilot Study. *J. Exp. Orthop.* 4 (14), 14–18. doi:10.1186/s40634-017-008910.1186/s40634-017-0089-1

Bernstein, A., Niemeyer, P., Salzmann, G., Südkamp, N. P., Hube, R., Klehm, J., et al. (2013). Microporous Calcium Phosphate Ceramics as Tissue Engineering Scaffolds for the Repair of Osteochondral Defects: Histological Results. *Acta Biomater.* 9 (7), 7490–7505. doi:10.1016/j.actbio.2013.03.021

Betsch, M., Thelen, S., Santak, L., Herten, M., Jungbluth, P., Miersch, D., et al. (2014). The Role of Erythropoietin and Bone Marrow Concentrate in the Treatment of Osteochondral Defects in Mini-Pigs. *Plos. ONE.* 9 (3), e92766–10. doi:10.1371/journal.pone.0092766

Blanke, M., Carl, H. D., Klinger, P., Swoboda, B., Hennig, F., and Gelse, K. (2009). Transplanted Chondrocytes Inhibit Endochondral Ossification within Cartilage Repair Tissue. *Calcif. Tissue Int.* 85 (421), 421–433. doi:10.1007/s00223-009-9288-9

Bozkurt, M., Aşık, M. D., Gürsoy, S., Türk, M., Karahan, S., Gümüşkaya, B., et al. (2019). Autologous Stem Cell-Derived Chondrocyte Implantation with Bio-Targeted Microspheres for the Treatment of Osteochondral Defects. *J. Orthop. Surg. Res.* 14 (394), 2–13. doi:10.1186/s13018-019-1434-0

Cancedda, R., Giannoni, P., and Mastrogiacomo, M. (2007). A Tissue Engineering Approach to Bone Repair in Large Animal Models and in Clinical Practice. *Biomaterials* 28 (29), 4240–4250. doi:10.1016/j.biomaterials.2007.06.023

Carneiro, M. d. O., Barbieri, C. H., and Barbieri Neto, J. (2013). O gel de plasma rico em plaquetas propicia a regeneração da cartilagem articular Do joelho de ovelhas. *Acta Ortop. Bras.* 21 (2), 80–86. doi:10.1590/S1413-78522013000200003

Chu, C. R., Szczodry, M., and Bruno, S. (2010). Animal Models for Cartilage Regeneration and Repair. *Tissue Eng. B: Rev.* 16 (1), 105–115. doi:10.1089/ten.teb.2009.0452

Davis, S., Roldo, M., Blunn, G., Tozzi, G., and Roncada, T. (2021). Influence of the Mechanical Environment on the Regeneration of Osteochondral Defects. *Front. Bioeng. Biotechnol.* 9, 1–23. doi:10.3389/fbioe.2021.603408

De Paz-Lugo, P., Lupiáñez, J. A., and Meléndez-Hevia, E. (2018). High glycine Concentration Increases Collagen Synthesis by Articular Chondrocytes *In Vitro*: Acute glycine Deficiency Could Be an Important Cause of Osteoarthritis. *Amino Acids* 50 (10), 1357–1365. doi:10.1007/s00726-018-2611-x

Deng, C., Chang, J., and Wu, C. (2019). Bioactive Scaffolds for Osteochondral Regeneration. *J. Orthopaedic Translation* 17 (45), 15–25. doi:10.1016/j.jot.2018.11.006

Dhollander, A., Sánchez, V., Almqvist, K., VerdonkVerbruggen, R. G., Verbruggen, G., and Verdonk, P. (2012). The Use of Scaffolds in the Treatment of Osteochondral Lesions in the Knee: Current Concepts and Future Trends. *J. Knee. Surg.* 25 (3), 179–186. doi:10.1055/s-0032-1322596

Higa, K., Kitamura, N., Goto, K., Kurokawa, T., Gong, J. P., Kanaya, F., et al. (2017). Effects of Osteochondral Defect Size on Cartilage Regeneration Using a Double-Network Hydrogel. *BM.C Musculoskelet. Disord.* 18 (210), 1–9. doi:10.1186/s12891-017-1578-1

Ho, S. T. B., Hutmacher, D. W., Ekaputra, A. K., Hitendra, D., and Hui, J. H. (2010). The Evaluation of a Biphasic Osteochondral Implant Coupled with an Electrospun Membrane in a Large Animal Model. *Tissue Eng. A* 16 (4), 1123–1141. doi:10.1089/ten.tea.2009.0471

Intema, F., Thomas, T. P., Anderson, D. D., Elkins, J. M., Brown, T. D., Amendola, A., et al. (2011). Subchondral Bone Remodeling Is Related to Clinical Improvement after Joint Distraction in the Treatment of Ankle Osteoarthritis. *Osteoarthritis and Cartilage* 19 (6), 668–675. doi:10.1016/j.joca.2011.02.005

Jainudeen, M. R., Wahid, H., and Hafez, E. S. E. (2000). "Ovulation Induction, Embryo Production and Transfer," in *Reproduction in Farm Animals*. Editors E. S. E. Hafez and B. Hafez (Baltimore): Lippincott Williams & Wilkins.), 421–430.

Junqueira, L. C., and Carneiro, J. (2005). "Connective Tissue," in *Basic Histology, Text & Atlas*. Editors L. C. Junqueira and J. Carneiro (; United States): McGraw-Hill Education), 151–178.

Karna, E., Szoka, L., HuynhPalka, T. Y. L. J. A., and Palka, J. A. (2020). Proline-dependent Regulation of Collagen Metabolism. *Cell. Mol. Life Sci.* 77 (10), 1911–1918. doi:10.1007/s00018-019-03363-3

Kim, T., See, C. W., Li, X., and Zhu, D. (2020). Orthopedic Implants and Devices for Bone Fractures and Defects: Past, Present and Perspective. *Engineered Regen.*, 1, 6–18. doi:10.1016/j.engreg.2020.05.003

Kon, E., Filardo, G., Roffi, A., Andriolo, L., and Marcacci, M. (2012). New Trends for Knee Cartilage Regeneration: From Cell-free Scaffolds to Mesenchymal Stem Cells. *Curr. Rev. Musculoskelet. Med.* 5 (3), 236–243. doi:10.1007/s12178-012-9135-x

Kresakova, L., Danko, J., Vdoviakova, K., Medvecky, L., Zert, Z., Petrovova, E., et al. (2021). *In Vivo* Study of Osteochondral Defect Regeneration Using Innovative Composite Calcium Phosphate Biocement in a Sheep Model. *Materials* 14 (16), 1–21. doi:10.3390/ma14164471

Leja, K., and Lewandowicz, G. (2010). Polymer Biodegradation and Biodegradable Polymers-A Review. *Pol. J. Environ. Stud.* 19 (2), 255–266.

Liu, Y., Zhou, G., and Cao, Y. (2017). Recent Progress in Cartilage Tissue Engineering-Our Experience and Future Directions. *Engineering* 3 (1), 28–35. doi:10.1016/J.ENG.2017.01.010

Lydon, H., Getgood, A., and Henson, F. M. D. (2019). Healing of Osteochondral Defects via Endochondral Ossification in an Ovine Model. *Cartilage* 10 (1), 94–101. doi:10.1177/1947603517713818

Macfadyen, M. A., Daniel, Z., Kelly, S., Parr, T., Brameld, J. M., Murton, A. J., et al. (2019). The Commercial Pig as a Model of Spontaneously-Occurring Osteoarthritis. *BMC. Musculoskelet. Disord.* 20 (1), 1–12. doi:10.1186/s12891-019-2452-0

Madry, H., Gao, L., Eichler, H., Orth, P., and Cucchiarini, M. (2017). Bone Marrow Aspirate Concentrate- Enhanced Marrow Stimulation of Chondral Defects. *Hindawi. Stem Cell Int.*, 1–13. doi:10.1155/2017/1609685

Maglio, M., Brogini, S., Pagani, S., Giavaresi, G., and Tschon, M. (2019). Current Trends in the Evaluation of Osteochondral Lesion Treatments: Histology, Histomorphometry, and Biomechanics in Preclinical Models. *Biomed. Res. Int.* 2019 (23), 1–27. doi:10.1155/2019/4040236

Mainil-Varlet, P., Aigner, T., Brittberg, M., Bullough, P., Hollander, A., Hunziker, E., et al. (2003). Histological Assessment of Cartilage Repair. *The J. Bone Jt. Surgery-American Volume* 85 (2), 45–57. doi:10.2106/00004623-200300002-00007

Malda, J., Groll, J., and van Weeren, P. R. (2019). Rethinking Articular Cartilage Regeneration Based on a 250-Year-Old Statement. *Nat. Rev. Rheumatol.* 15 (10), 571–572. doi:10.1038/s41584-019-0278-7

Mano, J. F., and Reis, R. L. (2007). Osteochondral Defects: Present Situation and Tissue Engineering Approaches. *J. Tissue Eng. Regen. Med.* 1 (4), 261–271. doi:10.1002/term.37

Mathis, D. T., Kaelin, R., Rasch, H., Arnold, M. P., and Hirschmann, M. T. (2018). Good Clinical Results but Moderate Osseointegration and Defect Filling of a Cell-free Multi-Layered Nano-Composite Scaffold for Treatment of Osteochondral Lesions of the Knee. *Knee Surg. Sports Traumatol. Arthrosc.* 26, 1273–1280. doi:10.1007/s00167-017-4638-z

Matricali, G. A., Dereymaeker, G. P., and Luyten, F. P. (2010). Donor Site Morbidity after Articular Cartilage Repair Procedures: A Review. *Acta Orthop. Belg.* 76 (5), 669–674.

Medvecky, L., Giretova, M., Stulajterova, R., Danko, J., Vdoviakova, K., Kresakova, L., et al. (2021). Characterization of Properties, *In Vitro* and *In Vivo* Evaluation of Calcium Phosphate/Amino Acid Cements for Treatment of Osteochondral Defects. *Materials* 14 (2), 1–27. doi:10.3390/ma14020436

Meng, X., Ziadlou, R., Grad, S., Alini, M., Wen, C., Lai, Y., et al. (2020). Animal Models of Osteochondral Defect for Testing Biomaterials. *Biochem. Res. Int.* 2020, 1–12. doi:10.1155/2020/9659412

Murata, D., Akieda, S., Misumi, K., and Nakayama, K. (2018). Osteochondral Regeneration with a Scaffold-free Three-Dimensional Construct of Adipose

Tissue-Derived Mesenchymal Stromal Cells in Pigs. *Tissue Eng. Regen. Med.* 15 (1), 101–113. doi:10.1007/s13770-017-0091-9

Özmeriç, A., Alemdaroglu, K. B., and Aydogan, N. H. (2014). Treatment for Cartilage Injuries of the Knee with a New Treatment Algorithm. *Wjo* 5 (5), 677–684. doi:10.5312/wjo.v5.i5.677

Pearce, A., Richards, R. G., Richards, R., Milz, S., Schneider, E., and Pearce, S. (2007). Animal Models for Implant Biomaterial Research in Bone: a Review. *eCM* 13 (13), 1–10. doi:10.22203/ecm.v013a01

Pilichi, S., Rocca, S., Pool, R. R., Dattena, M., Masala, G., Mara, L., et al. (2014). Treatment with Embryonic Stem-like Cells into Osteochondral Defects in Sheep Femoral Condyles. *BMC Vet. Res.* 10 (301), 1–12. doi:10.1186/s12917-014-0301-9

Pulliainen, O., Vasara, A. I., Hyttinen, M. M., Tiitu, V., Valonen, P., Kellomäki, M., et al. (2007). Poly-L-D-Lactic Acid Scaffold in the Repair of Porcine Knee Cartilage Lesions. *Tissue Eng.* 13 (6), 1347–1355. doi:10.1089/ten.2006.0347

Reinholz, G. G., Lu, L., Saris, D. B., Yaszemski, M. J., and O'Driscoll, S. W. (2004). Animal Models for Cartilage Reconstruction. *Biomaterials* 25 (9), 1511–1521. doi:10.1016/s0142-9612(03)00498-8

Rodrigues, M. B., and Camanho, G. L. (2010). MRI Evaluation of Knee Cartilage. *Revista Brasileira de Ortopedia (English Edition)* 45 (4), 340–346. doi:10.1016/S2255-4971(15)30379-7

Salkeld, S. L., Patron, L. P., Lien, J. C., Cook, S. D., and Jones, D. G. (2016). Biological and Functional Evaluation of a Novel Pyrolytic Carbon Implant for the Treatment of Focal Osteochondral Defects in the Medial Femoral Condyle: Assessment in a Canine Model. *J. Orthop. Surg. Res.* 11 (155), 1–12. doi:10.1186/s13018-016-0488-5

Shepherd, D. E. T., and Seedhom, B. B. (1999). Thickness of Human Articular Cartilage in Joints of the Lower Limb. *Ann. Rheum. Dis.* 58 (1), 27–34. doi:10.1136/ard.58.1.27

Shimomura, K., Ando, W., Tateishi, K., Nansai, R., Fujie, H., Hart, D. A., et al. (2010). The Influence of Skeletal Maturity on Allogenic Synovial Mesenchymal Stem Cell-Based Repair of Cartilage in a Large Animal Model. *Biomaterials* 31 (31), 8004–8011. doi:10.1016/j.biomaterials.2010.07.017

Smith, G. D., Knutsen, G., and Richardson, J. B. (2005). A Clinical Review of Cartilage Repair Techniques. *The J. Bone Jt. Surg. Br. volume* 87-B (4), 445–449. doi:10.1302/0301-620X.87B4.15971

Tamaddon, M., Gilja, H., Wang, L., Oliveira, J. M., Sun, X., Tan, R., et al. (2020). Osteochondral Scaffolds for Early Treatment of Cartilage Defects in Osteoarthritic Joints: from Bench to Clinic. *Biomater. Transl.* 1 (1), 3–17. doi:10.3877/cma.j.issn.2096-112X.2020.01.002

Van den Borne, M. P. J., Raijmakers, N. J. H., Vanlauwe, J., Victor, J., De Jong, S. N., Bellemans, J., et al. (2007). International Cartilage Repair Society (ICRS) and Oswestry Macroscopic Cartilage Evaluation Scores Validated for Use in Autologous Chondrocyte Implantation (ACI) and Microfracture. *Osteoarthritis and Cartilage* 15 (12), 1397–1402. doi:10.1016/j.joca.2007.05.005

Vilela, C. A., Correia, C., Oliveira, J. M., Sousa, R. A., Espregueira-Mendes, J., and Reis, R. L. (2015). Cartilage Repair Using Hydrogels: a Critical Review of *In Vivo* Experimental Designs. *ACS Biomater. Sci. Eng.* 1 (9), 726–739. doi:10.1021/acsbiomaterials.5b00245

Vindas Bolaños, R. A., Cokelaere, S. M., Estrada McDermott, J. M., Benders, K. E. M., Gbureck, U., Plomp, S. G. M., et al. (2017). The Use of a Cartilage Decellularized Matrix Scaffold for the Repair of Osteochondral Defects: the Importance of Long-Term Studies in a Large Animal Model. *Osteoarthritis and Cartilage* 25 (3), 413–420. doi:10.1016/j.joca.2016.08.005

Wang, W., and Yeung, K. W. K. (2017). Bone Grafts and Biomaterials Substitutes for Bone Defect Repair: A Review. *Bioactive Mater.* 2 (4), 224–247. doi:10.1016/j.bioactmat.2017.05.007

Widuchowski, W., Widuchowski, J., and Trzaska, T. (2007). Articular Cartilage Defects: Study of 25,124 Knee Arthroscopies. *The Knee* 14 (3), 177–182. doi:10.1016/j.knee.2007.02.001

Yen, Y.-M., Cascio, B., O'Brien, L., Stalzer, S., Millett, P. J., and Steadman, J. R. (2008). Treatment of Osteoarthritis of the Knee with Microfracture and Rehabilitation. *Med. Sci. Sports Exerc.* 40 (2), 200–205. doi:10.1249/mss.0b013e31815cb212

Yucekul, A., Ozdil, D., Kutlu, N. H., Erdemli, E., Aydin, H. M., and Doral, M. N. (2017). Tri-layered Composite Plug for the Repair of Osteochondral Defects: *In Vivo* Study in Sheep. *J. Tissue Eng.* 8 (8), 204173141769750–10. doi:10.1177/2041731417697500

ZhangMing, J. D., Ming, D., Ji, Q., Liu, A., Zhang, C., Jiao, J., et al. (2020). Repair of Osteochondral Defect Using Icariin-Conditioned Serum Combined with Chitosan in Rabbit Knees. *BMC Complement. Med. Ther.* 20193, 1–9. doi:10.1186/s12906-020-02996-3

Zlotnick, H. M., Locke, R. C., Stoeckl, B. D., Patel, J. M., Gupta, S., Browne, K. D., et al. (2021). Marked Differences in Local Bone Remodeling in Response to Different Marrow Stimulation Techniques in a Large Animal. *Eur. Cell Mater.* 1–16. doi:10.1101/2021.02.26.433037

Conflict of Interest: The authors declare that the research was conducted in the absence of any commercial or financial relationships that could be construed as a potential conflict of interest.

Publisher's Note: All claims expressed in this article are solely those of the authors and do not necessarily represent those of their affiliated organizations, or those of the publisher, the editors, and the reviewers. Any product that may be evaluated in this article, or claim that may be made by its manufacturer, is not guaranteed or endorsed by the publisher.